American Mineralogist, Volume 79, pages 789–792, 1994

Prediction of a high-pressure phase transition in Al_2O_3

Frederic C. Marton
Department of Geological Sciences, Northwestern University, 1847 Sheridan Road, Evanston, Illinois 60208-2150, U.S.A.
Ronald E. Cohen
Geophysical Laboratory and Center for High Pressure Research, Carnegie Institution of Washington, 5251 Broad Branch Road, NW, Washington, DC 20015-1305, U.S.A.

Abstract

A phase transition is predicted at high pressure (90 GPa) from the corundum structure to the Rh_2O_3(II) structure using first-principles calculations with the linearized, augmented plane-wave (LAPW) method. These results show that free Al_2O_3 in the deep lower mantle is unlikely to be in the form of corundum, although Al_2O_3 is probably not sufficiently abundant to give an observable signal in seismological data at the depth of a phase transition. The transition should also affect the fluorescence of Cr^{3+}-doped corundum (ruby), used as a pressure calibrant in diamond-anvil experiments, and should affect shock experiments using Al_2O_3 as a window material.

Introduction

Corundum appears to be stable over a wide pressure range, from 0 to over 175 GPa (Jephcoat et al., 1988) and has many experimental applications. It is used as a pressure calibrant in static high-pressure diamond-anvil experiments by fluorescence of Cr^{3+}-doped corundum, or ruby (Bell et al., 1984; Mao et al., 1986; Xu et al., 1986), and as a window material in dynamic high-pressure shock-wave experiments (Nellis and Yoo, 1990; Yoo et al., 1992). However, ionic models for corundum suggest that the mineral undergoes a phase change at moderate to high pressures. Energy calculations with the potential induced breathing model (PIB) predicted a transition to the Rh_2O_3(II) (*Pbna*) structure (Shannon and Prewitt, 1970) at a pressure of 6 or 62 GPa, depending on whether the Thomas-Fermi (TF) or Kohn-Sham (KS) form of the kinetic energy functional is used, respectively (Cynn et al., 1990). More recently, variationally induced breathing (VIB) model calculations predicted the same transition at 169 GPa (M.S.T. Bukowinski, 1994 personal communication). The PIB model also shows an elastic instability in corundum at high pressures (Cohen, 1987). The present calculations using the LAPW method (Wei and Krakauer, 1985; Singh, 1991) make no assumptions about ionicity, bonding, or form of the charge density and thus should be much more accurate and reliable than the simple ionic models.

In spite of many high-pressure experiments using corundum, there have been no definitive observations of phase transitions. The failure to observe a high-pressure Al_2O_3 polymorph in static room-temperature experiments may simply be due to metastable persistence of the corundum structure and sluggishness of the transformation at low temperatures. However, dynamic experiments that do reach high temperatures have also failed to show any direct evidence of a phase transition (Ahrens, 1980), but some have noted an increase in the optical opacity of Al_2O_3 in both the low and high pressure ranges (Urtiew, 1974; Yoo et al., 1992), and Yoo et al. (1992) observed an increase in the thermal emission at pressures of 200 GPa, which suggests a phase transition.

With an increase in the number of high-temperature diamond-anvil experiments, it becomes crucial to know whether corundum transforms at high pressures and temperatures because a different phase would most likely shift the fluorescence bands at a given pressure. Thus the pressures obtained by ruby fluorescence after heating may actually be fluorescence of the new phase and not of ruby.

The LAPW calculations make no approximations other than the local density approximation (LDA), which has been shown to be very accurate for other ionic oxides such as MgO (Mehl et al., 1986, 1988), SiO_2 (Cohen, 1991, 1992), and $MgSiO_3$ (Stixrude and Cohen, 1993). We thus have confidence in the accuracy of the predictions presented here.

Calculations

In the present study, the LAPW + LO method was used (Singh, 1991), which uses extra localized orbitals in addition to the usual LAPW basis functions to provide extra variational freedom in the muffin-tin spheres. This allows us to use a single energy window to treat both semicore and valence states accurately.

Calculations were done for corundum, with a set of six volumes between 29 and 48 Å^3 pfu. Corundum is rhombohedral, with space group $R\bar{3}c$ and ten atoms per primitive cell. Five volumes between 31 and 44 Å^3 pfu were used for Rh_2O_3(II), which is orthorhombic (space group *Pbna*), with 20 atoms per primitive cell. Structural parameters and atomic positions were taken from the PIB

Table 1. LAPW experimental parameters

	Mesh	k points	RK_{max}	Basis/atom	R_{MT} (Bohr)
		Corundum			
LAPW1	2 × 2 × 2	2	7.0	~98	1.55
LAPW2	4 × 4 × 4	10	7.5	~118	1.55
		Rh_2O_3(II)			
LAPW1	2 × 2 × 2	1	7.0	~93	1.55
LAPW2	4 × 4 × 4	8	7.5	~113	1.55

Table 3. Equation of state parameters for Rh_2O_3(II) (*Pbna*)

	PIB (KS)*	LAPW1		LAPW2	
Fit order	3	3	4	3	4
V_0 (Å³)	40.56	40.80	40.78	40.84	40.84
K_0 (GPa)	359	262	260	261	262
K_0'	4.01	4.03	4.48	3.97	3.88
K_0'' (GPa⁻¹)			−0.036		−0.011

Note: prime denotes pressure derivative. V_0 is the volume for one formula unit.
* Cynn et al. (1990).

calculations of Cynn et al. (1990). For corundum, these parameters were then corrected to match the experimental data of d'Amour et al. (1978) and Finger and Hazen (1978) by constant shifts. In the case of Rh_2O_3(II), no corrections were made since no experimental data are available. Any inaccuracy in the Rh_2O_3(II) parameters leads to an overestimation of its free energy, and thus an overestimation of the transition pressure.

To test for convergence, two sets of calculations were performed for each structure (Table 1). In the first set (LAPW1), a special **k**-point set of a 2 × 2 × 2 mesh was used in conjunction with a plane-wave cutoff of RK_{max} = 7.0. This gave two **k** points for corundum and one **k** point for Rh_2O_3(II) in the Brillouin zone, with approximately 98 and 93 basis functions per atom for each, respectively. In the second set (LAPW2), a 4 × 4 × 4 mesh and RK_{max} = 7.5 generated ten **k** points and approximately 118 basis functions per atom for corundum and eight **k** points and approximately 113 basis functions per atom for Rh_2O_3(II). Experience has shown that such tests are entirely sufficient to demonstrate convergence. The comparison indicates that energy differences in the LAPW2 results are fully converged, and the figures show only the fully converged results. The muffin-tin radii R_{MT} were 1.55 Bohr for both Al and O. For Al, 1s and 2s and, for O, 1s were treated as core states.

Results and discussion

The results of each set of calculations were fitted to third- and fourth-order Birch-Murnaghan equations of state (EOS) (Birch, 1978) and compared with experimental data (in the case of corundum) and PIB results (Tables 2 and 3). The values of the zero-pressure volume (V_0) for corundum match the experimental value of d'Amour et al. (1978) well, being within about 2%, and thermal corrections would give fortuitously perfect agreement. The bulk moduli are also in excellent agreement with adiabatic values determined by means of ultrasonic methods. Gieske and Barsch (1968) and Goto et al. (1989) both gave values of K_S = 254 GPa at ambient pressure and temperature, and Chung and Simmons (1968) gave K_S = 257 GPa at 1 atm and 4.2 K, matching our value. Figure 1 shows the relationship between internal energy and volume per formula unit of Al_2O_3 using a fourth-order fit to the Birch-Murnaghan equation for the LAPW2 data. The maximum errors in these fits are approximately 1 × 10^{-3} eV for corundum and 2 × 10^{-6} eV for Rh_2O_3(II), approximately the same as the estimated computational error in our calculations.

Figure 2 shows the equations of state for the two structures. The high-pressure results of Jephcoat et al. (1988) are nonhydrostatic and show a curvature that neither is parallel to either of the EOS curves, nor matches the low-pressure experimental data points. As they discussed, that

Table 2. Equation of state parameters for corundum $R\bar{3}c$

	EXP*	PIB (KS)**	LAPW1		LAPW2	
Fit order	3	3	3	4	3	4
V_0	42.65	41.56	41.79	41.74	41.80	41.79
K_0	254	356	262	262	257	257
K_0'	4.3	3.93	3.87	4.29	4.01	4.05
K_0''				−0.030		−0.016

Note: units for V_0, K_0, and K_0'' are Å³, GPa, and GPa⁻¹, respectively. Prime denotes pressure derivative. V_0 is the volume for one formula unit.
* Data from d'Amour et al. (1978).
** Data from Cynn et al. (1990).

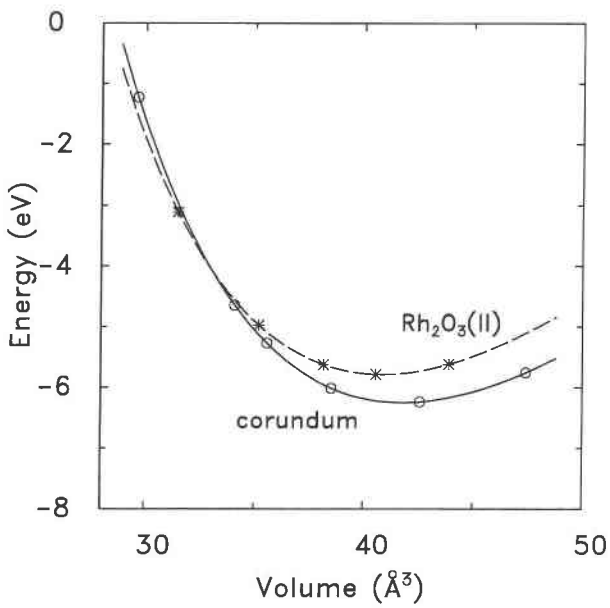

Fig. 1. LAPW2 internal energy as a function of volume per formula unit of Al_2O_3. The phase transition occurs at the common tangent of the two curves.

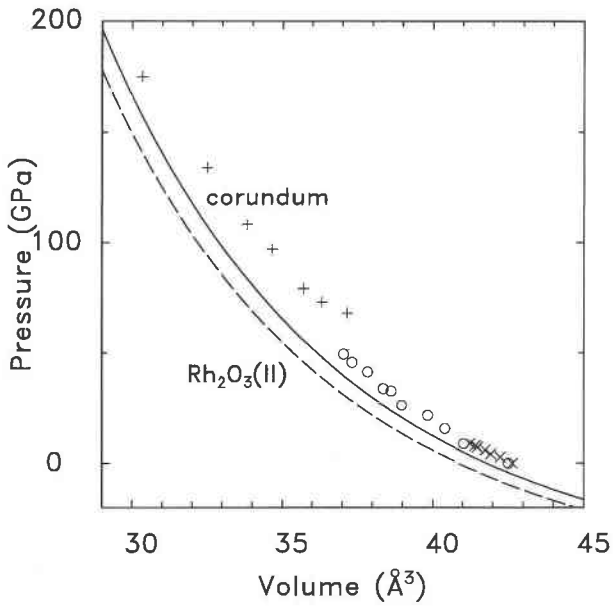

Fig. 2. Pressure vs. volume calculated from fourth-order Birch-Murnaghan equations of state for LAPW2 data. Symbols represent the experimental data for corundum: crosses = Jephcoat et al. (1988), open circles = Richet et al. (1988), × = d'Amour et al. (1978). Note that the data from Jephcoat et al. are nonhydrostatic and the data from Richet et al. are quasi-hydrostatic.

experiment was not designed to give an accurate equation of state; rather, they wished to search for a phase transition.

By calculating the enthalpy ($E + PV$) of the phases, we find the pressure at which a first-order phase transition occurs at low temperatures. Comparison of enthalpy were made for corresponding EOS fits for both sets of calculations, and the results are given in Table 4. Errors were estimated by changing the Rh_2O_3(II) energies by ±2 mRy pfu and recalculating the EOS and transition pressures. The LAPW1 transition pressures are 86 GPa for both third- and fourth-order Birch-Murnaghan fits to the data, whereas the third- and fourth-order LAPW2 fits both give 91 GPa. Free Al_2O_3 is therefore unlikely to be in the form of corundum in the deep lower mantle, although Al_2O_3 is probably not sufficiently abundant to give an observable seismological signal. Both sets of calculations give transition pressures higher than the PIB (KS) value of 62 GPa. These results again support the Kohn-Sham kinetic energy as being more accurate in the PIB ionic model for determinations of phase transitions than the Thomas-Fermi kinetic energy (Isaak et al., 1990). Estimates of the change in volume are comparable with the ionic calculations, near −2%. A similar phase transition was observed in a sample of Rh_2O_3 that was quenched at 1200–1500 °C and 6.5 GPa by Shannon and Prewitt (1970) that also had a ΔV of −2%.

The AlO_6 octahedra are quite regular in the corundum structure, with Al-O distances at zero pressure of 1.86 and 1.97 Å, with Al on the threefold symmetry axis. By comparison, the octahedra in the Rh_2O_3(II) structure are rather deformed, with six Al-O distances ranging from 1.83 to 2.05 Å and no symmetry at the Al site. Therefore the two fluorescence bands in ruby should split in Rh_2O_3(II). However, at gigapascal pressures, the splitting is unlikely to be resolved. Rather, one would expect a change in the shape of the bands, and the peak position would likely change at the transition at a given pressure.

TABLE 4. Phase transition data

	Third-order fit	Fourth-order fit
	PIB (KS)*	
Pressure (GPa)	62	
ΔV (%)	−2.3	
	LAPW1	
Pressure (GPa)	86 ± 6	86 ± 6
ΔV (%)	−2.15	−2.25
	LAPW2	
Pressure (GPa)	91 ± 6	91 ± 6
ΔV (%)	−2.16	−2.17

* Cynn et al. (1990).

ACKNOWLEDGMENTS

We thank Craig R. Bina for suggesting this project, and Kathleen Kingma and Lars Stixrude for helpful discussions. Mark S.T. Bukowinski generously shared his latest results and gave helpful comments on the manuscript, as did Mark Woods, Tom Shoberg, and an anonymous reviewer. F.C.M. began this work while he was a Visiting Investigator at the Geophysical Laboratory, Carnegie Institution of Washington, and was supported by NSF grant EAR-9158594 (CRB). R.E.C. acknowledges support from NSF grant EAR-9117932. Calculations were performed on the Convex C3 and Cray Y-MP at the National Center for Supercomputing Applications at the University of Illinois at Urbana-Champaign.

REFERENCES CITED

Ahrens, T.J. (1980) Dynamic compression of Earth materials. Science, 207, 1035–1041.

Bell, P.M., Mao, H.K., and Goettel, K. (1984) Ultrahigh pressure: Beyond 2 megabars and the ruby fluorescence scale. Science, 226, 542–544.

Birch, F. (1978) Finite strain isotherm and velocities for single-crystal and polycrystalline NaCl at high pressures and 300°K. Journal of Geophysical Research, 83, 1257–1268.

Chung, D.H., and Simmons, G. (1968) Pressure and temperature dependence of the isotropic elastic moduli of polycrystalline alumnia. Journal of Applied Physics, 39, 5316–5326.

Cohen, R.E. (1987) Calculation of elasticity and high pressure instabilities in corundum and stishovite with the potential induced breathing model. Geophysical Research Letters, 14, 37–40.

——— (1991) Bonding and elasticity of stishovite SiO_2 at high pressure: Linearized augmented plane wave calculations. American Mineralogist, 76, 733–742.

——— (1992) First-principles predictions of elasticity and phase transitions in high pressure SiO_2 and geophysical implications. In Y. Syono and M.H. Manghnani, Eds., High-pressure research: Application to Earth and planetary sciences, p. 425–431. American Geophysical Union, Washington, DC.

Cynn, H., Isaak, D.G., Cohen, R.E., Nicol, M.F., and Anderson, O.L. (1990) A high-pressure phase transition of corundum predicted by the potential induced breathing model. American Mineralogist, 75, 439–442.

d'Amour, H., Schiferl, D., Denner, W., Schultz, H., and Holzapfel, W.B. (1978) High-pressure single-crystal structure determinations for ruby

up to 90 kbar using an automatic diffractometer. Journal of Applied Physics, 49, 4411–4416.

Finger, L.W., and Hazen, R.M. (1978) Crystal structure and compression of ruby to 46 kbar. Journal of Applied Physics, 49, 5823–5826.

Gieske, J.H., and Barsch, G.R. (1968) Pressure dependence of the elastic constants of single crystalline aluminum oxide. Physica Status Solidi, 29, 121–131.

Goto, T., Anderson, O.L., Ohno, I., and Yamamoto, S. (1989) Elastic constants of corundum up to 1825 K. Journal of Geophysical Research, 94, 7588–7602.

Isaak, D.G., Cohen, R.E., and Mehl, M.J. (1990) Calculated elastic and thermal properties of MgO at high pressures and temperatures. Journal of Geophysical Research, 95, 7055–7067.

Jephcoat, A.P., Hemley, R.J., and Mao, H.K. (1988) X-ray diffraction of ruby (Al_2O_3:Cr^{3+}) to 175 GPa. Physica B, 150, 115–121.

Mao, H.K., Xu, J., and Bell, P.M. (1986) Calibration of the ruby pressure gauge of 800 kbar under quasi-hydrostatic conditions. Journal of Geophysical Research, 91, 4673–4676.

Mehl, M.J., Hemley, R.J., and Boyer, L.L. (1986) Potential-induced breathing model for the elastic moduli and high-pressure behavior of the cubic alkaline-earth oxides. Physical Review B, 33, 8685–8696.

Mehl, M.J., Cohen, R.E., and Krakauer, H. (1988) Linearized augmented plane wave electronic structure calculations for MgO and CaO. Journal of Geophysical Research, 93, 8009–8022.

Nellis, W.J., and Yoo, C.S. (1990) Issues concerning shock temperature measurements of iron and other metals. Journal of Geophysical Research, 95, 21749–21752.

Richet, P., Xu, J.A., and Mao, H.K. (1988) Quasi-hydrostatic compression of ruby to 500 kbar. Physics and Chemistry and Minerals, 16, 207–211.

Shannon, R.D., and Prewitt, C.T. (1970) Synthesis and structure of a new high-pressure form of Rh_2O_3. Journal of Solid State Chemistry, 2, 134–136.

Singh, D. (1991) Ground-state properties of lanthanum: Treatment of extended-core states. Physical Review B, 43, 6388–6392.

Stixrude, L., and Cohen, R.E. (1993) Stability of orthorhombic $MgSiO_3$ perovskite in the Earth's lower mantle. Nature, 364, 613–616.

Urtiew, P.A. (1974) Effect of shock loading on transparency of sapphire crystals. Journal of Applied Physics, 45, 3490–3493.

Wei, S.-H., and Krakauer, H. (1985) Local-density-functional calculation of the pressure-induced metallization of BaSe and BaTe. Physical Review Letters, 55, 1200–1203.

Xu, J., Mao, H.K., and Bell, P.M. (1986) High-pressure ruby and diamond fluorescence: Observations at 0.21 to 0.55 Terapascal. Science, 232, 1404–1406.

Yoo, C.S., Holmes, N.C., and See, E. (1992) Shock-induced optical changes in Al_2O_3 at 200 GPa: Implications for shock temperature measurements in metals. In S. Schmidt, R.D. Dick, J.W. Forbes, and D.G. Pasker, Eds., Shock compression of condensed matter—1991, p. 733–736. North-Holland, Amsterdam.

Manuscript received April 20, 1994
Manuscript accepted June 10, 1994